Cell Reports

Report

Reduced α-MSH Underlies Hypothalamic ER-Stress-Induced Hepatic Gluconeogenesis

Graphical Abstract

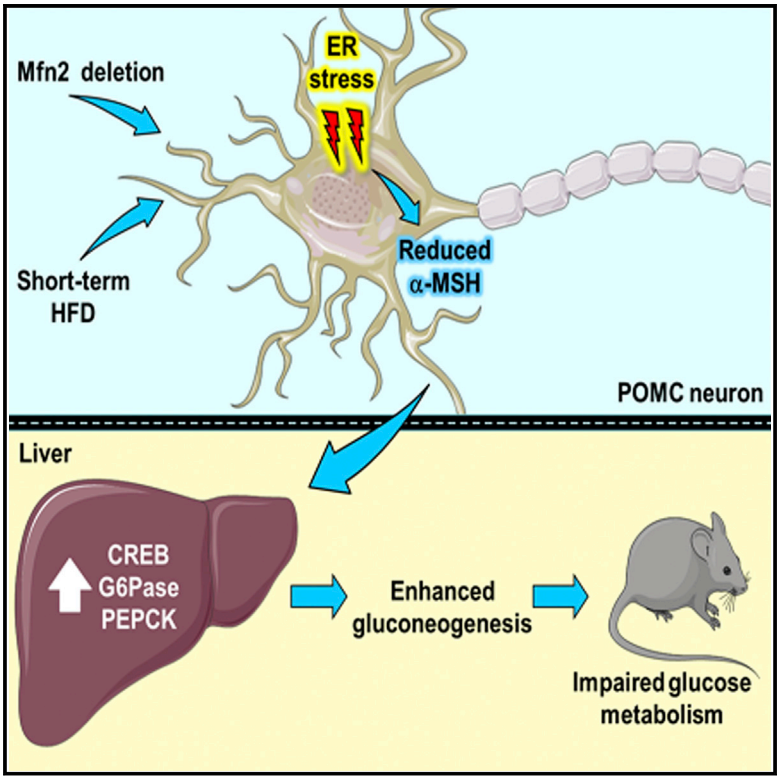

Authors

Marc Schneeberger, Alicia G. Gómez-Valadés, Jordi Altirriba, ..., Antonio Zorzano, Ramon Gomis, Marc Claret

Correspondence

mclaret@clinic.ub.es

In Brief

Alterations in ER homeostasis have been implicated in the pathophysiology of obesity and diabetes. Schneeberger et al. report that hypothalamic ER stress is associated with glucose homeostasis perturbations due to increased hepatic gluconeogenesis in mice. Defective α-MSH production underlies this phenotype, suggesting that α-MSH is a fundamental gluconeogenesis regulator.

Highlights

- Hypothalamic ER stress is associated with enhanced hepatic gluconeogenesis
- Defective α-MSH processing underlies increased hepatic glucose production
- Hypothalamic ER stress relief reverses glucose metabolism alterations

Accession Numbers

GSE62263

Schneeberger et al., 2015, Cell Reports *12*, 361–370
July 21, 2015
http://dx.doi.org/10.1016/j.celrep.2015.06.041

CellPress

Cell Reports
Report

Reduced α-MSH Underlies Hypothalamic ER-Stress-Induced Hepatic Gluconeogenesis

Marc Schneeberger,[1,2,3,10] Alicia G. Gómez-Valadés,[1,3,10] Jordi Altirriba,[4] David Sebastián,[3,5,6] Sara Ramírez,[1] Ainhoa Garcia,[1,3] Yaiza Esteban,[1,3] Anne Drougard,[1] Albert Ferrés-Coy,[8,9] Analía Bortolozzi,[8,9] Pablo M. Garcia-Roves,[1,3] John G. Jones,[7] Bruno Manadas,[7] Antonio Zorzano,[3,5,6] Ramon Gomis,[1,2,3] and Marc Claret[1,3,*]
[1]Diabetes and Obesity Research Laboratory, Institut d'Investigacions Biomèdiques August Pi i Sunyer (IDIBAPS), 08036 Barcelona, Spain
[2]Department of Endocrinology and Nutrition, Hospital Clínic, School of Medicine, University of Barcelona, 08036 Barcelona, Spain
[3]CIBER de Diabetes y Enfermedades Metabólicas Asociadas (CIBERDEM), Spain
[4]Laboratory of Metabolism, Department of Internal Medicine Specialties, Faculty of Medicine, University of Geneva, 1211 Geneva, Switzerland
[5]Institute for Research in Biomedicine (IRB Barcelona), 08028 Barcelona, Spain
[6]Departament de Bioquímica i Biologia Molecular, Facultat de Biologia, Universitat de Barcelona, 08028 Barcelona, Spain
[7]CNC—Center for Neuroscience and Cell Biology, University of Coimbra, 3060-197 Cantanhede, Portugal
[8]Department of Neurochemistry and Neuropharmacology, IIBB–CSIC–IDIBAPS, 08036 Barcelona, Spain
[9]Centro de Investigación Biomédica en Red de Salud Mental (CIBERSAM), 28029 Madrid, Spain
[10]Co-first author
*Correspondence: mclaret@clinic.ub.es
http://dx.doi.org/10.1016/j.celrep.2015.06.041

SUMMARY

Alterations in ER homeostasis have been implicated in the pathophysiology of obesity and type-2 diabetes (T2D). Acute ER stress induction in the hypothalamus produces glucose metabolism perturbations. However, the neurobiological basis linking hypothalamic ER stress with abnormal glucose metabolism remains unknown. Here, we report that genetic and induced models of hypothalamic ER stress are associated with alterations in systemic glucose homeostasis due to increased gluconeogenesis (GNG) independent of body weight changes. Defective alpha melanocyte-stimulating hormone (α-MSH) production underlies this metabolic phenotype, as pharmacological strategies aimed at rescuing hypothalamic α-MSH content reversed this phenotype at metabolic and molecular level. Collectively, our results posit defective α-MSH processing as a fundamental mediator of enhanced GNG in the context of hypothalamic ER stress and establish α-MSH deficiency in proopiomelanocortin (POMC) neurons as a potential contributor to the pathophysiology of T2D.

INTRODUCTION

Perturbations in ER performance, and the subsequent development of ER stress, have been implicated in the pathophysiology of metabolic disorders such as obesity and type-2 diabetes (T2D) (Ozcan et al., 2004, 2006). In particular, the hypothalamus has emerged as a key area of the CNS, causally linking ER stress, leptin resistance, and overweight (Cakir et al., 2013; Contreras et al., 2014; Hosoi et al., 2008; Ozcan et al., 2009; Won et al., 2009; Zhang et al., 2008). We have recently reported that the cellular responses to ER stress are modulated by Mitofusin 2 (Mfn2) (Muñoz et al., 2013; Schneeberger et al., 2013; Sebastián et al., 2012), a GTPase-containing mitochondrial protein that plays a prominent role in establishing mitochondria-ER contacts (de Brito and Scorrano, 2008). Consistently, mice lacking *Mfn2* in hypothalamic proopiomelanocortin (POMC) neurons (*POMCMfn2KO*), a subpopulation of anorexigenic neurons critical for energy and glucose homeostasis regulation (Grayson et al., 2013; Schneeberger et al., 2014), exhibited an obesogenic phenotype due to early ER-stress-induced leptin resistance (Schneeberger et al., 2013).

Albeit the connection between hypothalamic ER stress and obesity is well established, its potential contribution to the development of glucose homeostasis alterations irrespective of body weight has been scarcely investigated. Pharmacological and genetic studies indicate that ER stress pathways in the hypothalamus, and in POMC neurons, regulate whole-body glucose metabolism (Purkayastha et al., 2011; Williams et al., 2014). However, the precise molecular downstream mediators remain undefined.

Here, we explored the mechanisms by which hypothalamic POMC neurons, in the context of ER stress, contribute to systemic glucose metabolism disturbances. To this aim, we studied genetic and induced mouse models that develop early hypothalamic ER stress. Our results establish alpha-melanocyte-stimulating hormone (α-MSH), a neuropeptide derived from POMC processing, as a key mediator of hypothalamic ER-stress-induced hepatic gluconeogenesis (GNG) independent of obesity.

RESULTS

Deletion of *Mfn2* in POMC Neurons Leads to Systemic Alterations in Glucose Homeostasis Independently of Obesity Development

Twelve-week-old *POMCMfn2KO* mice exhibit a dramatic obese phenotype caused by hyperphagia and reduced thermogenesis.

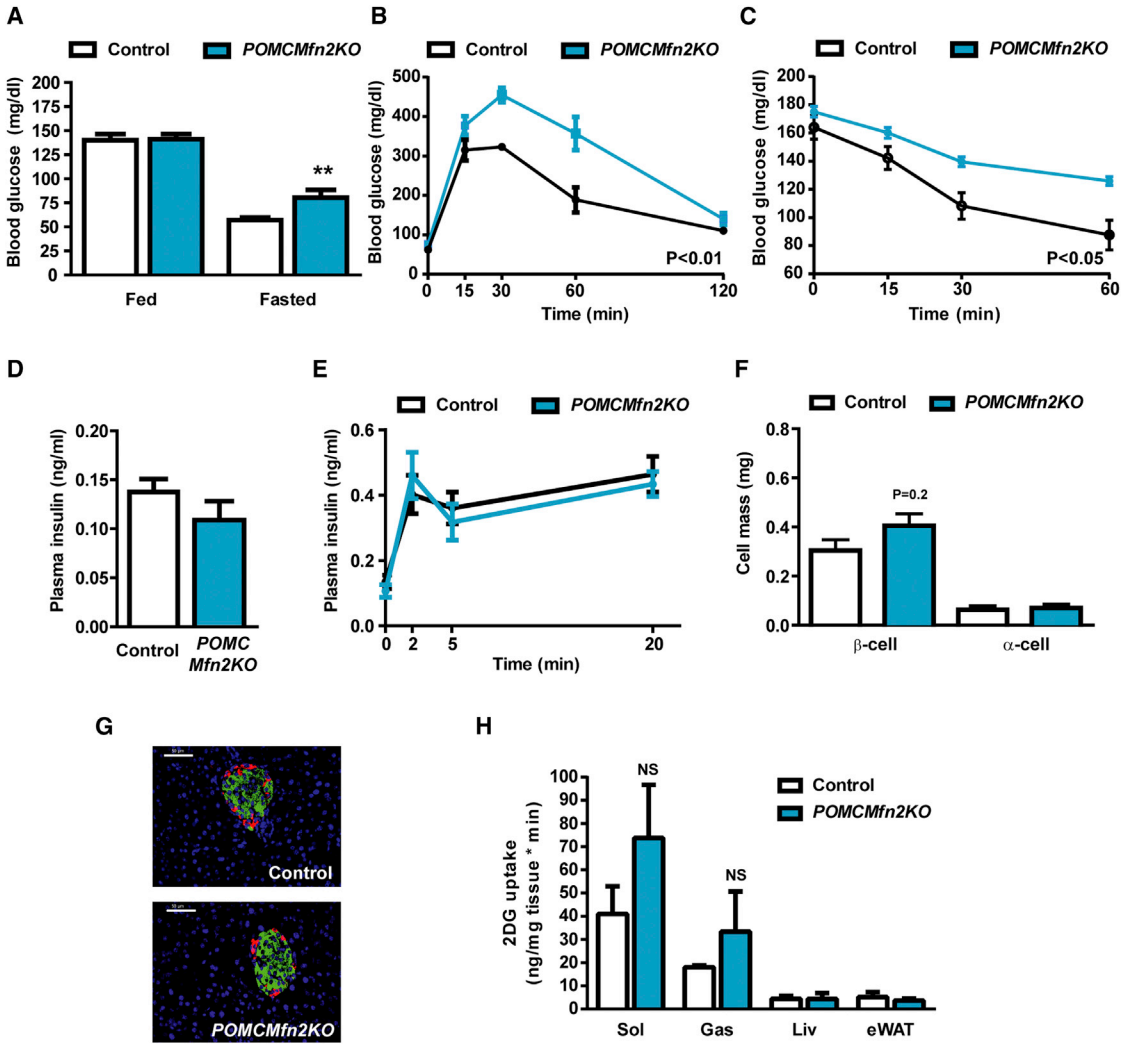

Figure 1. Defective Glucose Homeostasis in Weight-Matched *POMCMfn2KO* Mice Is Not Caused by Pancreatic Defects

(A–C) Fed and fasted glycemia (A), glucose tolerance (B), and insulin sensitivity (C) tests in control (n = 9–10) and *POMCMfn2KO* (n = 7–9) mice.

(D and E) Plasma insulin (D) and in vivo GSIS (E) in control (n = 10) and *POMCMfn2KO* (n = 7) mice.

(F and G) Pancreatic beta/alpha cell mass (F) and representative fluorescence images (G) of pancreatic islets (n = 3/genotype).

(H) Tissue-specific glucose uptake in soleus muscle (Sol), gastrocnemius muscle (Gas), liver (Liv), and epididymal white adipose tissue (eWAT) in control (n = 3) and *POMCMfn2KO* (n = 4) mice.

Data are expressed as mean ± SEM. **p < 0.01. NS, not significant. The scale bar represents 50 μm. See also Figure S1.

As expected, these mice showed marked alterations in glucose homeostasis including hyperglycemia, hyperinsulinemia, glucose intolerance, and insulin resistance (Schneeberger et al., 2013; Figures S1A–S1D).

To discriminate whether abnormal glucose homeostasis was a primary defect or secondary to obesity, we performed subsequent studies in 6-week-old *POMCMfn2KO* mice when no differences in body weight or adiposity were recorded (Schneeberger et al., 2013). Weight-matched *POMCMfn2KO* mice exhibited fasting hyperglycemia (Figure 1A), glucose intolerance (Figure 1B), and insulin resistance (Figure 1C). Together, these results demonstrate defective glucose control in *POMCMfn2KO* mice irrespective of body weight.

Increased Hepatic Glucose Production in Young Weight-Matched *POMCMfn2KO* Mice

Pancreatic β-cell dysfunction may cause abnormal glucose homeostasis. However, no alterations in plasma insulin (Figure 1D), glucose-stimulated insulin secretion (GSIS) (Figure 1E), pancreatic islet architecture, and number (control: 46 ± 9 islets/cm^2 versus *POMCMfn2KO*: 60 ± 6 islets/cm^2; NS; n = 3/genotype) or pancreatic α/β-cell mass (Figures 1F and 1G) were observed in 6-week-old weight-matched *POMCMfn2KO* mice, indicating normal pancreatic islet mass and function.

To assess the contribution of individual insulin-sensitive tissues to the development of glucose metabolism perturbations in *POMCMfn2KO* mice, we measured in vivo glucose uptake

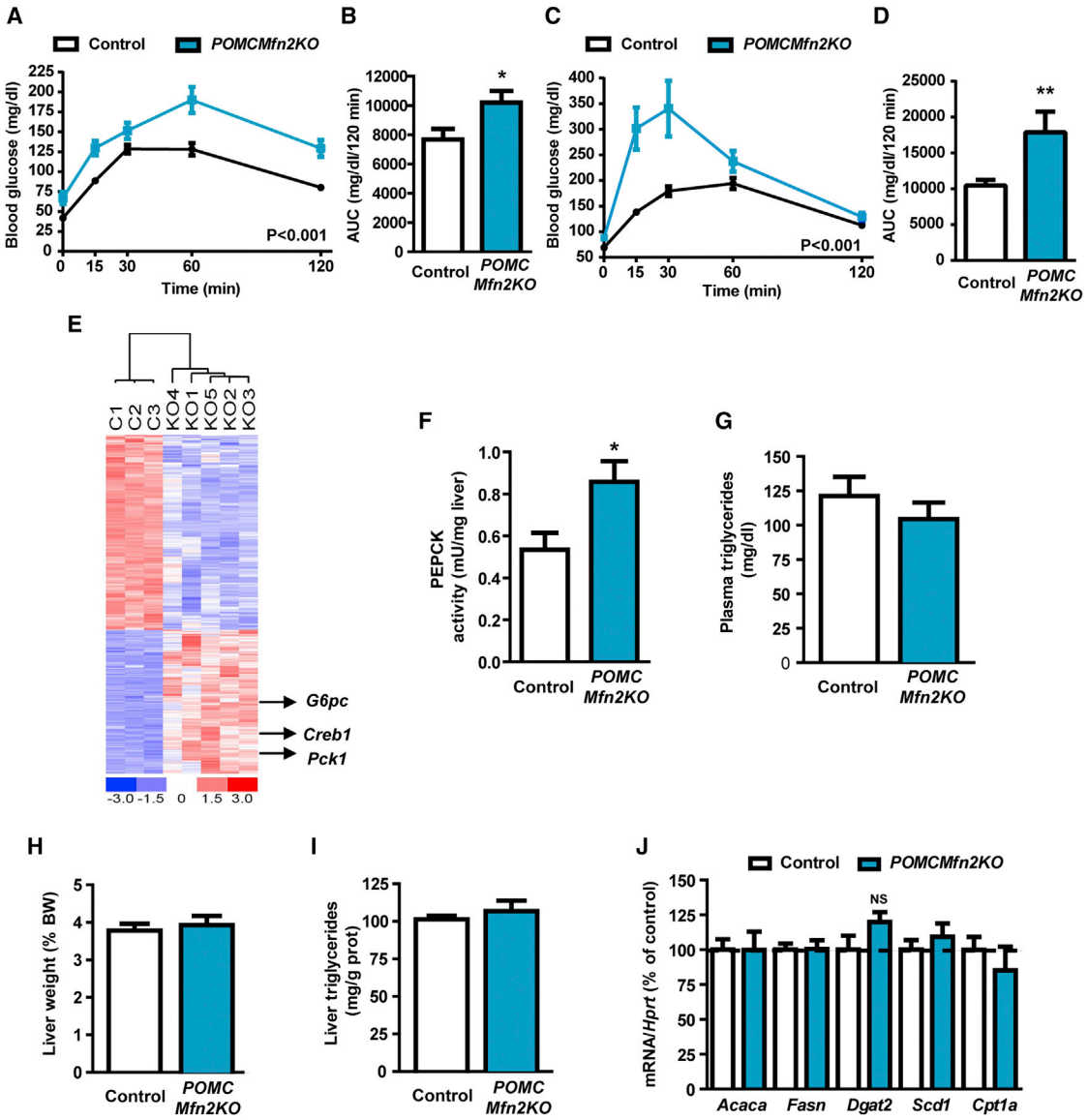

Figure 2. Enhanced Hepatic GNG in Weight-Matched *POMCMfn2KO* Mice

(A–D) Pyruvate tolerance test (A) and area under the curve (AUC) (B) and glycerol tolerance test (C) and AUC (D) of control (n = 9–11) and *POMCMfn2KO* (n = 5–7) mice.

(E) Heatmap representation of relative gene expression changes in livers from control (n = 3) and *POMCMfn2KO* (n = 4) mice.

(F) PEPCK activity in liver homogenates from control (n = 9) and *POMCMfn2KO* (n = 15) mice.

(G) Plasma triglyceride concentration in control (n = 6) and *POMCMfn2KO* (n = 8) mice.

(H and I) Liver weight (H) and triglyceride content (I) in control (n = 6) and *POMCMfn2KO* (n = 7) mice.

(J) Expression of key lipid metabolism genes in livers from control and *POMCMfn2KO* mice (n = 6/genotype). *Hprt* was used as housekeeping gene.

Data are expressed as mean ± SEM. BW, body weight. *p < 0.05. See also Figure S2 and Tables S1 and S2.

following a glucose load. 2-[^{3}H]deoxyglucose (2DG) uptake in *POMCMfn2KO* mice was similar to control counterparts in all tested tissues, although a non-significant trend to exhibit higher values in skeletal muscle was observed in mutant mice (Figure 1H). Nevertheless, this observation could not explain the impaired glucose homeostasis observed in *POMCMfn2KO* mice and it could represent a secondary compensatory mechanism.

The liver is a major regulator of whole-body glucose homeostasis through hepatic glucose production (HGP). Pyruvate tolerance test (PTT) and glycerol tolerance tests (GlyTTs) were used to assess HGP due to the difficulty to perform hyperinsulinemic-euglycemic clamps at such a young age (4 weeks). *POMCMfn2KO* mice displayed significantly higher blood glucose levels (Figures 2A–2D), suggestive of enhanced HGP.

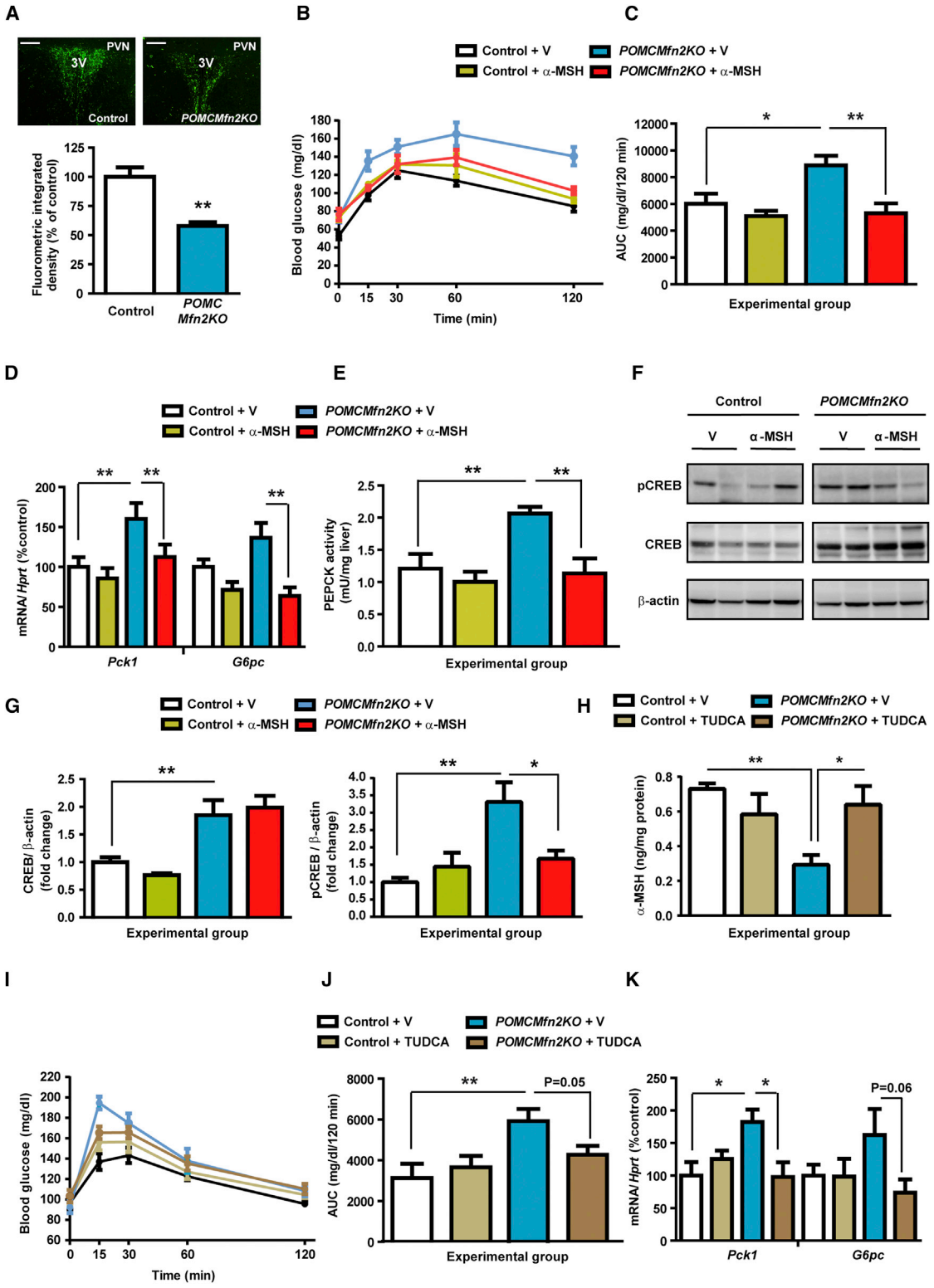

Figure 3. Reduced α-MSH Underlies Hypothalamic ER-Stress-Induced Hepatic GNG in *POMCMfn2KO* Mice

(A) Immunofluorescence images showing α-MSH staining in the PVN from 6-week-old control and *POMCMfn2KO* mice and integrated density quantification (n = 3/genotype). 3V, third ventricle.

(legend continued on next page)

In an attempt to determine the hepatic molecular alterations leading to enhanced GNG, we performed a global transcriptomic analysis in livers from young weight-matched *POMCMfn2KO* and control mice (Table S1). To establish relevant dysregulated pathways, we conducted associated disease analyses. The most highly enriched category was "nutritional and metabolic diseases," with 535 transcripts significantly altered (Figure S2A; Table S2). A large proportion of these transcripts (62%) belonged to the subcategory "glucose metabolism disorders" (Figure S2B). Consistent with enhanced HGP, the expression of key hepatic gluconeogenic genes such as cAMP responsive element-binding protein 1 (*Creb1*), glucose 6-phosphatase (*G6pc*), and cytosolic phosphoenolpyruvate carboxykinase (*Pck1*) was increased in mutant mice (Figure 2E; Table S2). Overexpression of these genes was validated by qRT-PCR (Figure S2C). Hepatic phosphoenolpyruvate carboxykinase (PEPCK) enzyme activity was also increased in *POMCMfn2KO* mice (Figure 2F). No changes in liver glycogen content were observed (control: 2.85 ± 0.97 μg/mg liver versus *POMCMfn2KO*: 3.34 ± 0.76 μg/mg liver; NS; n = 15/genotype). These results suggest that enhanced GNG is a major contributor to altered glucose homeostasis in weight-matched *POMCMfn2KO* mice.

In contrast, hepatic lipid metabolism was unperturbed in mutant mice, as no changes in plasma triglycerides (Figure 2G), liver weight (Figure 2H), hepatic triglyceride concentration (Figure 2I), and expression of key enzymes such as acetyl-CoA carboxylase (*Acaca*), fatty acid synthase (*Fasn*), diacylglycerol acyltransferase 2 (*Dgat2*), stearoyl-coenzyme A desaturase 1 (*Scd1*), or carnitine palmitoyltransferase 1 (*Cpt1a*) were observed (Figure 2J).

Next, we assessed biological parameters of hypothalamic-pituitary-adrenal axis function. Plasma concentration of epinephrine (control: 23.6 ± 1.2 pg/ml versus *POMCMfn2KO*: 27.1 ± 2.7 pg/ml; NS; n = 5–7/genotype), norepinephrine (control: 235 ± 50 pg/ml versus *POMCMfn2KO*: 280 ± 47 pg/ml; NS; n = 5–7/genotype), adenocorticotropic hormone (control: 48.8 ± 7.1 pg/ml versus *POMCMfn2KO*: 76.3 ± 19.3 pg/ml; NS; n = 5–7/genotype), and corticosterone (basal control: 48.2 ± 12.3 pg/ml versus basal *POMCMfn2KO*: 68.3 ± 21.2 pg/ml; NS; n = 6–9/genotype; stressed control: 447 ± 25 pg/ml versus stressed *POMCMfn2KO*: 451 ± 35 pg/ml; NS; n = 6–9/genotype) was unaltered. Together, these results suggest that neither defective insulin counter-regulatory hormones nor hypothalamic-pituitary-adrenal axis function mediates the enhanced GNG observed in *POMCMfn2KO* mice.

Reduced α-MSH in *POMCMfn2KO* Mice Underlies Enhanced GNG

Hypothalamic POMC neurons release α-MSH, a critical neuropeptide implicated in energy balance and metabolic control (Schneeberger et al., 2014). Weight-matched 6-week-old *POMCMfn2KO* mice displayed decreased hypothalamic α-MSH content (Schneeberger et al., 2013) and staining in neuronal projections to target areas such as the paraventricular nucleus (PVN) (Figure 3A). To investigate whether augmented GNG resulted from reduced α-MSH production, we assessed the effects of intracerebroventricular (i.c.v.) administration of this peptide. Acute i.c.v. α-MSH delivery to *POMCMfn2KO* mice normalized GNG (Figures 3B and 3C). Consistently, expression of hepatic gluconeogenic enzymes *Pck1* and *G6pc* (Figure 3D), as well as PEPCK activity (Figure 3E), was restored after central α-MSH administration.

The Effects of α-MSH on HGP in *POMCMfn2KO* Mice Are Mediated by CREB

Transcriptome analysis identified *Creb1* as a differentially expressed gene in livers from *POMCMfn2KO* mice (Figures 2E and S2C). Key gluconeogenic genes, including *Pck1* and *G6pc*, contain cAMP responsive elements (CRE) (Altarejos and Montminy, 2011), and thus, we assessed whether *Creb1* mediated the effects of hypothalamic α-MSH on GNG. Consistent with transcriptomic data, liver homogenates from weight-matched 6-week-old *POMCMfn2KO* mice showed increased CREB protein content, which was unchanged after i.c.v. α-MSH administration (Figures 3F and 3G). CREB activity is mainly regulated by phosphorylation (Altarejos and Montminy, 2011). Liver phospho-CREB (pCREB) levels in *POMCMfn2KO* were also elevated (Figures 3F and 3G). Remarkably, acute i.c.v. α-MSH was able to normalize pCREB levels to control values (Figures 3F and 3G). To assess the relevance of these findings, we investigated the effects of the manipulation of CREB phosphorylation status using the PKA selective inhibitor Rp-cAMPS, which effectively inhibits GNG (Dragland-Meserve et al., 1986). *POMCMfn2KO* mice treated with Rp-cAMPS displayed a normalized PTT, consistent with reduced gluconeogenic capacity (Figure S3). Together, these results indicate that α-MSH deficiency in *POMCMfn2KO* mice leads to enhanced gluconeogenic programming mediated by CREB.

ER-Stress-Associated Reduction of α-MSH Is the Cause of Enhanced HGP in *POMCMfn2KO* Mice

Decreased α-MSH content, in the context of hypothalamic ER stress, is normalized after ER stress relief by central chaperone treatment (Cakir et al., 2013; Schneeberger et al., 2013). Thus, we evaluated the acute effects of i.c.v. delivery of the chemical chaperone tauroursodeoxycholic acid (TUDCA) on GNG in *POMCMfn2KO* mice. This treatment was able to normalize hypothalamic α-MSH content (Figure 3H) and ameliorated the gluconeogenic response to pyruvate in *POMCMfn2KO* mice (Figures

(B–E) Vehicle (V) or α-MSH were administered i.c.v. and PTT (B), its AUC (C), expression of hepatic gluconeogenic genes (D), and PEPCK activity (E) were assayed (n = 6/group).
(F) Liver immunoblots for CREB and pCREB expression after acute i.c.v. administration of V or α-MSH (n = 4/group). All samples were run on the same gel.
(G) Densitometric quantification.
(H) Hypothalamic levels of α-MSH after acute central administration of V or TUDCA in control (n = 3–4/group) and *POMCMfn2KO* (n = 5/group) mice.
(I and J) PTT (I) and AUC (J) after central administration of V or TUDCA in control (n = 7/group) and *POMCMfn2KO* (n = 10/group) mice.
(K) Expression of hepatic gluconeogenic genes after central administration of V or TUDCA in control (n = 3–4/group) and *POMCMfn2KO* (n = 5/group) mice.
Data are expressed as mean ± SEM. *p < 0.05; **p < 0.01. The scale bar represents 100 μm. See also Figure S3.

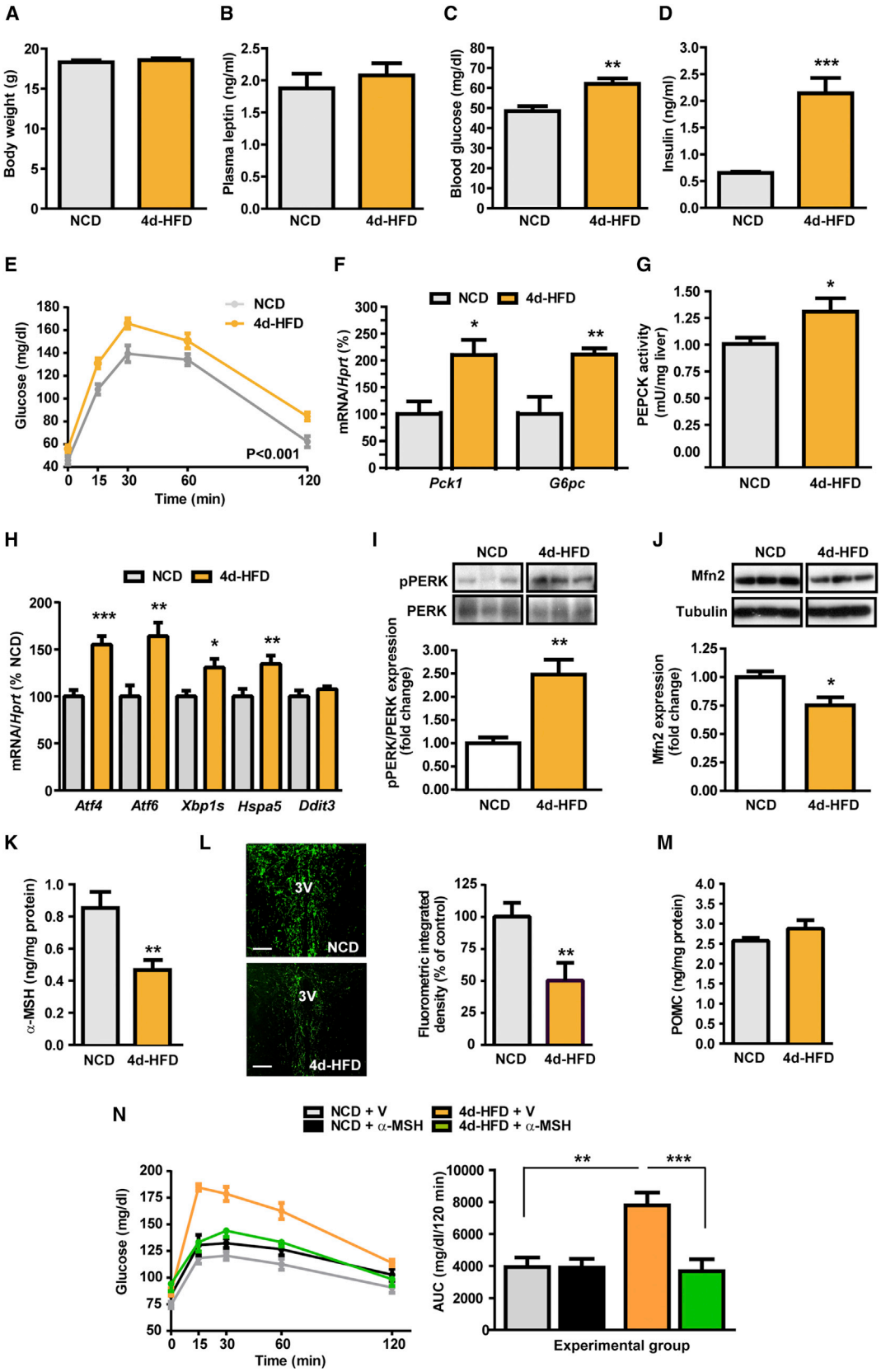

(legend on next page)

3I and 3J). Hepatic expression of gluconeogenic genes was also recovered after TUDCA administration (Figure 3K). Collectively, our data suggest that augmented GNG in *POMCMfn2KO* mice is the consequence of ER-stress-driven reduction of hypothalamic α-MSH levels.

Short-Term HFD Administration Causes ER-Stress-Mediated Reduction of Hypothalamic α-MSH Content and Enhanced HGP in the Absence of Obesity

The relevance of hypothalamic α-MSH in the regulation of GNG was further investigated in a pathophysiological model that recapitulates the effects of Western diets upon glucose homeostasis. To this end, we fed C57Bl/6J mice with high-fat diet for 4 consecutive days (4d-HFD), a sufficiently brief time interval to avoid weight gain as a possible confounding factor. Consistent with previous reports (Lee et al., 2011; Wang et al., 2001; Wiedemann et al., 2013), short-term HFD feeding caused no significant changes in body weight (Figure 4A) or plasma leptin levels (Figure 4B) but induced fasting hyperglycemia (Figure 4C), hyperinsulinemia (Figure 4D), and impaired pyruvate tolerance (Figure 4E) when compared to counterparts fed with normal chow diet (NCD). Consistently, increased expression of liver gluconeogenic genes (Figure 4F) and PEPCK activity (Figure 4G) were observed in 4d-HFD mice.

The molecular mechanisms underlying these rapid detrimental effects on glucose homeostasis after short-term HFD feeding are incompletely understood. We explored whether 4d-HFD regime was sufficient to enable ER stress in the hypothalamus of C57Bl/6J mice. We found that 4d-HFD feeding significantly increased the transcript expression of key ER stress markers, such as activating transcription factor 4 (*Atf4*) and 6 (*Atf6*), spliced form of X-box-binding protein 1 (*Xbp1s*), and binding immunoglobulin protein (*BiP*/*Hspa5*), suggesting enhanced hypothalamic ER stress (Figure 4H). Protein expression analysis of ER stress mediators in the hypothalamus from 4d-HFD mice also showed a significant increase of PERK phosphorylation (Figure 4I), which is a major transducer of the ER stress response in the hypothalamus (Ozcan et al., 2009), and a trend to increase in other ER stress markers (Figure S4A). Mfn2 expression was reduced in the hypothalamus of 4d-HFD (Figure 4J). Remarkably, the deleterious effects of short-term HFD were associated with reduced hypothalamic α-MSH content (Figure 4K) and fiber staining in neuronal projections to the PVN (Figure 4L) despite unaltered *Pomc* mRNA (NCD: 100% ± 13% versus 4d-HFD: 97% ± 12%; NS; n = 7/group), POMC protein content (Figure 4M), or POMC neuron number (NCD: 983 ± 40 versus 4d-HFD: 993 ± 76; NS; n = 3/group). The reduced α-MSH/POMC ratio suggests defective POMC processing. However, no changes in the transcript expression of the main POMC convertases were observed in the hypothalamus of 4d-HFD mice (Figure S4B). Given that proconvertase (PC) 1/3 and PC2 are regulated at protein level rather than mRNA level (Cakir et al., 2013), we conducted immunoblot analysis. Whereas PC1/3 expression was unchanged, PC2 levels were increased in the hypothalami from 4d-HFD mice (Figure S4C), likely as a compensatory mechanism to maintain adequate melanocortin tone.

To demonstrate a causal relationship between defective hypothalamic α-MSH levels and increased GNG, we conducted i.c.v. α-MSH administration studies. Acute delivery of α-MSH was able to restore pyruvate tolerance in 4d-HFD mice (Figure 4N).

DISCUSSION

Enhanced hepatic GNG is a major contributor of fasting hyperglycemia in T2D patients (DeFronzo et al., 1989; Magnusson et al., 1992). In addition to the classical hormonal regulatory mechanisms, the brain has long been recognized as a key regulator of this biological process (Bisschop et al., 2015) and hypothalamic POMC neurons have recently emerged as a relevant neuronal population implicated in the regulation of HGP (Berglund et al., 2012, 2013; Claret et al., 2011; Shi et al., 2013; Williams et al., 2014; Xu et al., 2010). Given that acute ER stress induction in the hypothalamus produces glucose metabolism alterations in a body-weight-independent manner (Purkayastha et al., 2011), we investigated the molecular link between ER stress in POMC neurons and glucose homeostasis.

We have recently reported that Mfn2 critically modulates cellular ER stress responses (Muñoz et al., 2013). Consistently, deletion of *Mfn2* leads to ER stress in vitro and in vivo (Ngoh et al., 2012; Schneeberger et al., 2013; Sebastián et al., 2012). In POMC neurons, Mfn2 deficiency causes an obesogenic phenotype characterized by early hypothalamic ER-stress-induced leptin resistance (Schneeberger et al., 2013). Remarkably, *POMCMfn2KO* mice exhibit abnormal glucose homeostasis before the onset of obesity due to enhanced GNG. Along the same lines, our short-term HFD model recapitulated the phenotypical outcome of *POMCMfn2KO* mice, defined by reduced hypothalamic Mfn2 expression, ER stress, and enhanced gluconeogenic capacity in the absence of changes in body weight.

Defective processing and production of α-MSH neuropeptide has been proposed to constitute the underlying neurobiological basis of hypothalamic ER stress in obesity (Cakir et al., 2013; Schneeberger et al., 2013). Similarly, 4 days of HFD administration also caused a reduction in hypothalamic α-MSH content and

Figure 4. Short-Term HFD Causes Enhanced GNG in the Absence of Obesity due to ER-Stress-Associated Reduction in α-MSH

(A–G) Effects of NCD or 4d-HFD in C57BL/6J mice on (A) body weight (n = 10/group), (B) plasma leptin (n = 8/group), (C) fasting blood glucose (n = 8/group), (D) plasma insulin (n = 8/group), (E) PTT (n = 10/group), (F) hepatic expression of gluconeogenic genes, and (G) PEPCK activity (n = 8/group).

(H) Hypothalamic mRNA expression of ER stress markers (n = 12/group).

(I and J) Hypothalamic PERK phosphorylation (n = 6/group; I) and Mfn2 protein levels (n = 6/group; J).

(K and L) Hypothalamic α-MSH content (n = 6/group; K) and immunofluorescence images showing α-MSH staining in the PVN from NCD or 4d-HFD mice and integrated density quantification (n = 3/genotype; L).

(M) Hypothalamic POMC content (n = 6/group).

(N) PTT and AUC after central administration of vehicle or α-MSH (n = 6 to 7/genotype/treatment).

Data are expressed as mean ± SEM. *p < 0.05; **p < 0.01; ***p < 0.001. The scale bar represents 100 μm.

fiber staining in the PVN. Even though abnormal α-MSH trafficking to target areas cannot be completely ruled out, the reduced α-MSH/POMC ratio suggests that defective POMC processing is the likeliest cause in both models studied. Our data also indicate that processing perturbations are the consequence of intrinsic factors (e.g., POMC protein misfolding) rather than defective PC expression.

In view of these results, it was reasonable to speculate that altered α-MSH content was also implicated in the development of inadequate glucose homeostasis in the context of hypothalamic ER stress. Indeed, our data demonstrate a causative involvement of α-MSH in the maintenance of systemic glucose homeostasis, as restoration of hypothalamic α-MSH levels, either by direct administration of this peptide and/or pharmacological ER stress relief, normalized HGP in these mouse models. The beneficial effects of the pharmacological treatment are likely mediated through direct actions on POMC neurons, although we cannot exclude potential effects on other hypothalamic areas due to the delivery route used.

The precise mechanisms by which hypothalamic α-MSH controls hepatic GNG are still incompletely understood, although a key mediator appears to be the modulation of CREB activity in the liver. CREB is considered a master positive regulator of gluconeogenic gene expression (Altarejos and Montminy, 2011; Erion et al., 2009; Herzig et al., 2001, 2003). However, conditional genetic ablation of *Creb1* in adult hepatocytes did not cause alterations in glucose metabolism or expression of gluconeogenic genes (Lee et al., 2014). This suggests functional redundancy, and thus we cannot exclude modulatory effects of α-MSH on other proteins that bind to CREs.

Extensive evidence indicates that the hypothalamus, and particularly the melanocortin system, regulates HGP through multisynaptic connections to autonomic centers (Bisschop et al., 2015). Recent studies have used genetic deletion and re-expression strategies to delineate the role of melanocortin signaling in sympathetic and parasympathetic preganglionic neurons (Berglund et al., 2014; Rossi et al., 2011). Reactivation of melanocortin 4 receptors (MCR4s), which bind α-MSH, in all cholinergic neurons attenuated hyperglycemia and hyperinsulinemia, whereas its selective re-expression in brainstem neurons was sufficient to improve hyperinsulinemia (Rossi et al., 2011). This suggests that MC4R signaling in cholinergic preganglionic sympathetic neurons mediates HGP suppression. This is consistent with our data demonstrating that reduced melanocortin tone in *POMCMfn2KO* or short-term HFD-fed mice is associated with increased GNG. The importance of the sympathetic outflow on the hypothalamic regulation of HGP is further supported by other studies (Purkayastha et al., 2011; van den Hoek et al., 2008). In this sense, preliminary results showed that prazosin (an alpha-1 adrenergic receptor blocker) was able to reverse enhanced HGP in *POMCMfn2KO* mice (M.S., A.G.G.-V., and M.C., unpublished data). Thus, it is tempting to speculate that α-MSH actions are mediated by sympathetic innervation, although the precise mechanisms by which POMC neurons propagate this signal remain unknown.

In summary, here we demonstrate that pathophysiological situations associated with hypothalamic ER stress cause systemic glucose homeostasis perturbations, named enhanced GNG, in the absence of obesity. We provide evidence that deficient α-MSH output, which is exclusively released by POMC neurons, is a critical mediator of hypothalamic ER-stress-induced GNG. These results provide further understanding of the central mechanisms involved in HGP regulation and establish α-MSH processing defects in POMC neurons as a potential contributor to the pathophysiology of T2D.

EXPERIMENTAL PROCEDURES

Mice and Diets

C57BL/6J mice were purchased from Harlan Europe. The generation of *POMCMfn2KO* mice has been previously reported (Schneeberger et al., 2013). Mice were maintained on a 12:12 hr light-dark cycle with free access to water and NCD (Harlan Research Laboratories) or HFD (45% kcal fat; Research Diets) for 4 days (starting at 6 weeks of age). *POMCMfn2KO* male mice were studied at 5 to 6 weeks of age or otherwise stated. In vivo studies were performed with approval of the University of Barcelona Ethics Committee, complying with current Spanish and European legislation.

Physiological Measurements

Blood samples were collected via tail vein or trunk bleeds using a capillary collection system (Sarstedt). Blood glucose was measured using a Glucometer (Arkray). GTT (D-glucose; 2 g/kg), GSIS (D-glucose; 3 g/kg), PTT (sodium pyruvate; 1 g/kg), and GlyTT (glycerol; 1 g/kg) were performed on overnight fasted mice. Insulin sensitivity tests (0.4 IU/kg) were performed on 6 hr food-deprived mice. All compounds were i.p. injected and blood glucose determined at the indicated time points. Plasma hormones were measured by commercially available ELISA kits in overnight fasted mice: insulin (Crystalchem); leptin (Crystalchem); epinephrine and norepinephrine (Labor Diagnostika Nord); adrenocorticotropic hormone (Abnova); and corticosterone (Immuno Diagnostic Systems). Plasma triglycerides were measured using quantitative enzymatic determination TAG kit (Sigma-Aldrich).

Hypothalamic POMC, α-MSH Content, and Immunohistochemistry

Mice were transcardially perfused with 4% paraformaldehyde, overnight fixed, cryoprotected in 30% sucrose, and frozen. Brains were cut into 25-μm-thick slices using a sliding microtome. Hypothalamic slices were extensively washed in KPBS buffer and blocked in 2% donkey serum in KPBS plus 0.4% Triton X-100. Sections were incubated with α-MSH antibody (1:20,000; Chemicon) or POMC antibody (1:1,000; Phoenix Pharmaceuticals) in blocking buffer for 48 hr at 4°C. After washing with KPBS, slices were incubated with the appropriate Alexa 488 antibody (1:400; Molecular Probes). Imaging was performed using a Leica DMI 6000B microscope. α-MSH integrated density after image skeletonization was calculated using ImageJ software. POMC neurons were counted in equivalent ARC sections (bregma −1.46 to −1.94). For α-MSH content, hypothalami were sonicated in 500 μl of 0.1 N HCl solution. Lysates were centrifuged and supernatants used for the quantification of α-MSH by ELISA (Phoenix Pharmaceuticals). Protein concentration was determined by Bradford.

qRT-PCR

Hypothalami and livers were harvested and immediately frozen in liquid nitrogen. mRNA was isolated using Trizol. Retrotranscription and qRT-PCR was performed as previously described (Claret et al., 2011). Transcript levels were measured using the ABI Prism 7900 HT system (Applied Biosystems). Proprietary Taqman Gene Expression assay FAM/TAMRA primers used (Applied Biosystems) were *Acaca* (Mm01304277_m1), *Atf4* (Mm00515324_m1), *Atf6* (Mm01295317_m1), *Cpe* (Mm00516341_m1), *Cpt1a* (Mm00550438_m1), *Creb1* (Mm00501607_m1), *Ddit3* (Mm00492097_m1), *Dgat2* (Mm00499536_m1), *Fasn* (Mm00662319_m1), *G6pc* (Mm00839363_m1), *Hprt* (Mm00446968_m1), *Hspa5* (Mm00517691_m1), *Pck1* (Mm00440636_m1), *Pcsk1* (Mm00479023_m1), *Pcsk2* (Mm00500981_m1), *Prcp* (Mm00804502_m1), *Scd1* (Mm01197142_m1), and *Xbp1s* (Mm03464496_m1).

Western Blot Analysis

Protein lysates were prepared from pulverized whole-liver samples or mediobasal hypothalamic microdissections in RIPA buffer (Sigma-Aldrich) supplemented with protease and phosphatase inhibitors. Cleared supernatants were resolved on pre-cast gradient 4%–12% SDS-PAGE gels (Bio-Rad), transferred onto PVDF membranes (Millipore), and probed with the following primary antibodies: phospho CREB (Ser133; 1:1,000; Cell Signaling Technology); CREB (1:1,000; Cell Signal); Mfn2 (1:1,000; Abcam); phospho PERK (1:1,000; Cell Signaling); PERK (1:1,000; Cell Signal); XBP1 (1:1,000; Abcam); p-eiF2α (1:1,000; Cell Signal); ATF4 (1:1,000; Aviva Systems Biology), ATF6 (1:1,000; Santa Cruz Biotechnology); CHOP (1:1,000; Santa Cruz); PC1 (1:5,000; MyBiosource); PC2 (1:5,000; MyBiosource), alpha-tubulin (1:8,000; Sigma-Aldrich); and beta-actin (1:5,000; Sigma-Aldrich). Detection was performed by enhanced chemiluminescence (Pierce). Band intensities were quantified using the ImageJ software.

i.c.v. Cannulation and Treatments

i.c.v. surgery was performed at 9 weeks of age as previously described (Schneeberger et al., 2013). On experimental days, 10-week-old control and *POMCMfn2KO* mice or C57BL/6J mice fed with NCD or HFD for 4 days were fasted overnight and infused with 2 μl of either vehicle (aCSF; Tocris Bioscience), α-MSH (1 nmol/μl; Sigma-Aldrich), or TUDCA (2.5 μg/μl; Calbiochem) just after lights on. Two hours later, a PTT was performed. For TUDCA experiments, an extra i.c.v. injection was performed just before fasting.

Statistics

Data are expressed as mean ± SEM. p values were calculated using unpaired Student's t test, two-way ANOVA, or one-way ANOVA with post hoc Sidak multiple comparisons test as appropriate. $p < 0.05$ was considered significant.

ACCESSION NUMBERS

The microarray data reported in this paper have been deposited to the NCBI GEO and are available under accession number GEO: GSE62263.

SUPPLEMENTAL INFORMATION

Supplemental Information includes Supplemental Experimental Procedures, four figures, and two tables and can be found with this article online at http://dx.doi.org/10.1016/j.celrep.2015.06.041.

AUTHOR CONTRIBUTIONS

M.S., A.G.G.-V., J.A., D.S., J.G.J., B.M., and M.C. designed and performed experiments and analyzed data. A.G., Y.E., S.R., A.F.-C., A.D., and A.B. performed experiments. P.M.G.-R., A.Z., and R.G. provided reagents and intellectual input. M.C. conceived the study, supervised research, and wrote the manuscript with input from all authors.

ACKNOWLEDGMENTS

We thank Gregory S. Barsh (Stanford University) for providing *Pomc-cre* mice and José C. Perales (University of Barcelona [UB]) and Claude Knauf (INSERM, Toulouse) for scientific advice. This work has been supported by grants PI10/01074 (to M.C.), PI13/01604 (to M.C.), and PI13/01390 (to A.B.; Plan Estatal de I+D+I 2013-2016) cofunded by ISCIII-Subdirección General de Investigación y Fomento de la Investigación el Fondo Europeo de Desarrollo Regional (FEDER); RecerCaixa 2010ACUP_00275 (to M.C.); Generalitat de Catalunya 2014SGR659 (to R.G.) and 2014SGR48 (to A.Z.); Ministerio de Ciencia y Competitividad SAF2013-40987R (to A.Z.); Marie Curie People Cofund Fellowship, Seventh Framework Programme of the European Commission grant 267248:DIATRAIN (to A.G.G.-V.); and co-funding from Fundação para a Ciência e a Tecnologia (FCT) and FEDER through COMPETE programme for grants REDE/1506/REM/2005 (National Mass Spectrometry Network), RECI/QEQ-QFI/0168/2012 (UC-NMR Center), EXCL/DTP-PIC/0069/2012, and structural funding for the Center for Neurosciences (PEst-C/SAU/LA0001/2011; to J.G.J. and B.M.). M.S. is a recipient of an undergraduate grant from the UB. A.F.-C. is a recipient of a fellowship from Spanish Ministry of Education, Culture and Sport. M.C. is a recipient of a Miguel Servet contract (MICINN-ISCIII; CP09/00233). P.M.G.-R. is a recipient of a Ramon y Cajal contract (MICINN; RYC-2009-05158). A.Z. is a recipient of an ICREA Acadèmia (Generalitat de Catalunya). This work was carried out in part at the Esther Koplowitz Centre.

Received: January 9, 2015
Revised: May 4, 2015
Accepted: June 10, 2015
Published: July 9, 2015

REFERENCES

Altarejos, J.Y., and Montminy, M. (2011). CREB and the CRTC co-activators: sensors for hormonal and metabolic signals. Nat. Rev. Mol. Cell Biol. *12*, 141–151.

Berglund, E.D., Vianna, C.R., Donato, J., Jr., Kim, M.H., Chuang, J.C., Lee, C.E., Lauzon, D.A., Lin, P., Brule, L.J., Scott, M.M., et al. (2012). Direct leptin action on POMC neurons regulates glucose homeostasis and hepatic insulin sensitivity in mice. J. Clin. Invest. *122*, 1000–1009.

Berglund, E.D., Liu, C., Sohn, J.W., Liu, T., Kim, M.H., Lee, C.E., Vianna, C.R., Williams, K.W., Xu, Y., and Elmquist, J.K. (2013). Serotonin 2C receptors in pro-opiomelanocortin neurons regulate energy and glucose homeostasis. J. Clin. Invest. *123*, 5061–5070.

Berglund, E.D., Liu, T., Kong, X., Sohn, J.W., Vong, L., Deng, Z., Lee, C.E., Lee, S., Williams, K.W., Olson, D.P., et al. (2014). Melanocortin 4 receptors in autonomic neurons regulate thermogenesis and glycemia. Nat. Neurosci. *17*, 911–913.

Bisschop, P.H., Fliers, E., and Kalsbeek, A. (2015). Autonomic regulation of hepatic glucose production. Compr. Physiol. *5*, 147–165.

Cakir, I., Cyr, N.E., Perello, M., Litvinov, B.P., Romero, A., Stuart, R.C., and Nillni, E.A. (2013). Obesity induces hypothalamic endoplasmic reticulum stress and impairs proopiomelanocortin (POMC) post-translational processing. J. Biol. Chem. *288*, 17675–17688.

Claret, M., Smith, M.A., Knauf, C., Al-Qassab, H., Woods, A., Heslegrave, A., Piipari, K., Emmanuel, J.J., Colom, A., Valet, P., et al. (2011). Deletion of Lkb1 in pro-opiomelanocortin neurons impairs peripheral glucose homeostasis in mice. Diabetes *60*, 735–745.

Contreras, C., González-García, I., Martínez-Sánchez, N., Seoane-Collazo, P., Jacas, J., Morgan, D.A., Serra, D., Gallego, R., Gonzalez, F., Casals, N., et al. (2014). Central ceramide-induced hypothalamic lipotoxicity and ER stress regulate energy balance. Cell Rep. *9*, 366–377.

de Brito, O.M., and Scorrano, L. (2008). Mitofusin 2 tethers endoplasmic reticulum to mitochondria. Nature *456*, 605–610.

DeFronzo, R.A., Ferrannini, E., and Simonson, D.C. (1989). Fasting hyperglycemia in non-insulin-dependent diabetes mellitus: contributions of excessive hepatic glucose production and impaired tissue glucose uptake. Metabolism *38*, 387–395.

Dragland-Meserve, C.J., Olivieri, M.C., and Botelho, L.H. (1986). Inhibition of hepatic gluconeogenesis by the Rp-diastereomer of adenosine cyclic 3′,5′-phosphorothioate. Biochem. J. *237*, 463–468.

Erion, D.M., Ignatova, I.D., Yonemitsu, S., Nagai, Y., Chatterjee, P., Weismann, D., Hsiao, J.J., Zhang, D., Iwasaki, T., Stark, R., et al. (2009). Prevention of hepatic steatosis and hepatic insulin resistance by knockdown of cAMP response element-binding protein. Cell Metab. *10*, 499–506.

Grayson, B.E., Seeley, R.J., and Sandoval, D.A. (2013). Wired on sugar: the role of the CNS in the regulation of glucose homeostasis. Nat. Rev. Neurosci. *14*, 24–37.

Herzig, S., Long, F., Jhala, U.S., Hedrick, S., Quinn, R., Bauer, A., Rudolph, D., Schutz, G., Yoon, C., Puigserver, P., et al. (2001). CREB regulates hepatic gluconeogenesis through the coactivator PGC-1. Nature *413*, 179–183.

Herzig, S., Hedrick, S., Morantte, I., Koo, S.H., Galimi, F., and Montminy, M. (2003). CREB controls hepatic lipid metabolism through nuclear hormone receptor PPAR-gamma. Nature *426*, 190–193.

Hosoi, T., Sasaki, M., Miyahara, T., Hashimoto, C., Matsuo, S., Yoshii, M., and Ozawa, K. (2008). Endoplasmic reticulum stress induces leptin resistance. Mol. Pharmacol. *74*, 1610–1619.

Lee, Y.S., Li, P., Huh, J.Y., Hwang, I.J., Lu, M., Kim, J.I., Ham, M., Talukdar, S., Chen, A., Lu, W.J., et al. (2011). Inflammation is necessary for long-term but not short-term high-fat diet-induced insulin resistance. Diabetes *60*, 2474–2483.

Lee, D., Le Lay, J., and Kaestner, K.H. (2014). The transcription factor CREB has no non-redundant functions in hepatic glucose metabolism in mice. Diabetologia *57*, 1242–1248.

Magnusson, I., Rothman, D.L., Katz, L.D., Shulman, R.G., and Shulman, G.I. (1992). Increased rate of gluconeogenesis in type II diabetes mellitus. A 13C nuclear magnetic resonance study. J. Clin. Invest. *90*, 1323–1327.

Muñoz, J.P., Ivanova, S., Sánchez-Wandelmer, J., Martínez-Cristóbal, P., Noguera, E., Sancho, A., Díaz-Ramos, A., Hernández-Alvarez, M.I., Sebastián, D., Mauvezin, C., et al. (2013). Mfn2 modulates the UPR and mitochondrial function via repression of PERK. EMBO J. *32*, 2348–2361.

Ngoh, G.A., Papanicolaou, K.N., and Walsh, K. (2012). Loss of mitofusin 2 promotes endoplasmic reticulum stress. J. Biol. Chem. *287*, 20321–20332.

Ozcan, U., Cao, Q., Yilmaz, E., Lee, A.H., Iwakoshi, N.N., Ozdelen, E., Tuncman, G., Görgün, C., Glimcher, L.H., and Hotamisligil, G.S. (2004). Endoplasmic reticulum stress links obesity, insulin action, and type 2 diabetes. Science *306*, 457–461.

Ozcan, U., Yilmaz, E., Ozcan, L., Furuhashi, M., Vaillancourt, E., Smith, R.O., Görgün, C.Z., and Hotamisligil, G.S. (2006). Chemical chaperones reduce ER stress and restore glucose homeostasis in a mouse model of type 2 diabetes. Science *313*, 1137–1140.

Ozcan, L., Ergin, A.S., Lu, A., Chung, J., Sarkar, S., Nie, D., Myers, M.G., Jr., and Ozcan, U. (2009). Endoplasmic reticulum stress plays a central role in development of leptin resistance. Cell Metab. *9*, 35–51.

Purkayastha, S., Zhang, H., Zhang, G., Ahmed, Z., Wang, Y., and Cai, D. (2011). Neural dysregulation of peripheral insulin action and blood pressure by brain endoplasmic reticulum stress. Proc. Natl. Acad. Sci. USA *108*, 2939–2944.

Rossi, J., Balthasar, N., Olson, D., Scott, M., Berglund, E., Lee, C.E., Choi, M.J., Lauzon, D., Lowell, B.B., and Elmquist, J.K. (2011). Melanocortin-4 receptors expressed by cholinergic neurons regulate energy balance and glucose homeostasis. Cell Metab. *13*, 195–204.

Schneeberger, M., Dietrich, M.O., Sebastián, D., Imbernón, M., Castaño, C., Garcia, A., Esteban, Y., Gonzalez-Franquesa, A., Rodríguez, I.C., Bortolozzi, A., et al. (2013). Mitofusin 2 in POMC neurons connects ER stress with leptin resistance and energy imbalance. Cell *155*, 172–187.

Schneeberger, M., Gomis, R., and Claret, M. (2014). Hypothalamic and brainstem neuronal circuits controlling homeostatic energy balance. J. Endocrinol. *220*, T25–T46.

Sebastián, D., Hernández-Alvarez, M.I., Segalés, J., Sorianello, E., Muñoz, J.P., Sala, D., Waget, A., Liesa, M., Paz, J.C., Gopalacharyulu, P., et al. (2012). Mitofusin 2 (Mfn2) links mitochondrial and endoplasmic reticulum function with insulin signaling and is essential for normal glucose homeostasis. Proc. Natl. Acad. Sci. USA *109*, 5523–5528.

Shi, X., Zhou, F., Li, X., Chang, B., Li, D., Wang, Y., Tong, Q., Xu, Y., Fukuda, M., Zhao, J.J., et al. (2013). Central GLP-2 enhances hepatic insulin sensitivity via activating PI3K signaling in POMC neurons. Cell Metab. *18*, 86–98.

van den Hoek, A.M., van Heijningen, C., Schröder-van der Elst, J.P., Ouwens, D.M., Havekes, L.M., Romijn, J.A., Kalsbeek, A., and Pijl, H. (2008). Intracerebroventricular administration of neuropeptide Y induces hepatic insulin resistance via sympathetic innervation. Diabetes *57*, 2304–2310.

Wang, J., Obici, S., Morgan, K., Barzilai, N., Feng, Z., and Rossetti, L. (2001). Overfeeding rapidly induces leptin and insulin resistance. Diabetes *50*, 2786–2791.

Wiedemann, M.S., Wueest, S., Item, F., Schoenle, E.J., and Konrad, D. (2013). Adipose tissue inflammation contributes to short-term high-fat diet-induced hepatic insulin resistance. Am. J. Physiol. Endocrinol. Metab. *305*, E388–E395.

Williams, K.W., Liu, T., Kong, X., Fukuda, M., Deng, Y., Berglund, E.D., Deng, Z., Gao, Y., Liu, T., Sohn, J.W., et al. (2014). Xbp1s in Pomc neurons connects ER stress with energy balance and glucose homeostasis. Cell Metab. *20*, 471–482.

Won, J.C., Jang, P.G., Namkoong, C., Koh, E.H., Kim, S.K., Park, J.Y., Lee, K.U., and Kim, M.S. (2009). Central administration of an endoplasmic reticulum stress inducer inhibits the anorexigenic effects of leptin and insulin. Obesity (Silver Spring) *17*, 1861–1865.

Xu, Y., Berglund, E.D., Sohn, J.W., Holland, W.L., Chuang, J.C., Fukuda, M., Rossi, J., Williams, K.W., Jones, J.E., Zigman, J.M., et al. (2010). 5-HT2CRs expressed by pro-opiomelanocortin neurons regulate insulin sensitivity in liver. Nat. Neurosci. *13*, 1457–1459.

Zhang, X., Zhang, G., Zhang, H., Karin, M., Bai, H., and Cai, D. (2008). Hypothalamic IKKbeta/NF-kappaB and ER stress link overnutrition to energy imbalance and obesity. Cell *135*, 61–73.